CALIBRATION OF SOIL DISCRETE ELEMENT CONTACT PARAMETER IN RHIZOME MEDICINAL MATERIALS PLANTING AREA IN HILLY REGION
/
丘陵山地根茎类中药材种植区土壤离散元参数标定

Bin CHEN[1)], Yan LIU[1)], Qingxu YU[1)], Xiaobing CHEN[1)], Youyi MIAO[1)], Yuanxiu HE[2)], Jiahao CHEN[3)], Jingchao ZHANG*[1)]

[1)] Nanjing Institute of Agricultural Mechanization, Ministry of Agriculture and Rural Affairs, Nanjing / China;
[2)] NanJing XiaoZhuang University, Nanjing / China;
[3)] HeFei Normal University, Hefei / China;
Tel: +86 025-84346278-60; E-mail: zhangjingchao@caas.cn
DOI: https://doi.org/10.35633/inmateh-68-51

Keywords: *rhizome medicinal materials; hilly region; soil discrete element parameters; calibration; soil-machine interaction*

ABSTRACT
Aiming at the lack of accurate and reliable discrete element simulation parameters in the study of the soil-machine interaction mechanism and the design of machinery in the planting areas of rhizomes in hilly mountainous areas, EDEM software was used to calibrate the parameters. The soil angle of repose test was used to calibrate the contact parameters between soil particles, and the soil sliding test was used to calibrate the contact parameters between soil and machinery. The Box-Behnken optimization method was used to establish the multiple regression model of the angle of repose and the sliding angle, and the optimal contact parameters between soil particles were obtained by solving the model. The optimal combination of contact parameters was used to conduct tests on the angle of repose and soil sliding angle and the errors between the simulation and physical tests were 3.94% and 3.66%, respectively. In order to further verify the accuracy of the calibrated and optimized discrete element model parameters, the rotary tillage ridge field test and the simulation test were used for comparative analysis, and the relative errors of the simulated test results and the field test results for ridge height, ridge top width, and ditch bottom width were obtained, respectively. 4.45%, 6.96%, 8.56%, the error is within the acceptable range. The rotary tillage and ridging effects are consistent in simulation and field tests, confirming the accuracy and reliability of the calibration of soil parameters.

摘要
针对丘陵山区根茎类中药材种植区土壤-机械互作机理研究以及机具设计缺乏准确可靠的离散元仿真参数的问题,采用 EDEM 软件进行参数标定。采用土壤休止角试验校准土壤颗粒之间的接触参数，采用土壤滑动试验校准土壤与机械之间的接触参数。采用 Box-Behnken 优化方法建立了静止角和滑动角的多元回归模型，通过解算模型得到土壤颗粒间的最佳接触参数。以最优组合进行堆积角试验和滑落角试验，仿真试验和物理试验之间的误差分别为 3.94%、3.66%。为进一步验证标定优化的离散元模型参数的准确性，采用旋耕起垄田间试验和仿真试验进行对比分析，获取垄高、垄顶宽、沟底宽仿真试验结果与田间试验结果的相对误差分别为 4.45%、6.96%、8.56%，误差在可接受范围内。仿真试验和田间试验旋耕起垄效果基本一致，验证了土壤参数标定的准确可靠。

INTRODUCTION
Chinese medicinal materials are a characteristic economic crop. In recent years, Chinese medicinal materials planting has become a pillar industry for rural revitalization. In China, the planting area of Chinese medicinal materials is about 5,864 thousand hectares *(Chen et al., 2021)*. However, the comprehensive mechanization rate of Chinese medicinal materials is only 16.87% *(Huang Luqi, 2021)*. Among them, rhizome medicinal materials have the most diverse varieties and highest production, while their production is also most labor-intensive and has the least mechanization rate *(Zhao et al., 2012)*. In order to improve the mechanization level of rhizome medicinal materials production, it is necessary to study the soil-machine interaction mechanism in planting area.

1 Bin Chen, ENGR; Yan Liu, Pro; Qingxu Yu, PHD student; Xiaobing Chen, Pro; Youyi Miao, ENGR; Yuanxiu He, BSC student; Jiahao Chen, BSC student; Jingchao Zhang, ENGR.

The discrete element method (DEM) has become an important means to study the mechanism of soil-machine interaction *(Ucgul et al., 2020)*. Different types of soil lead to differences in the performance of soil-mechanical interactions *(Chen et al., 2013).* When modeling different types of soil, it is necessary to select an appropriate soil contact model and accurately calibrate the relevant model parameters according to the specific conditions of the soil to ensure the authenticity of the simulation test. Aitkins et al. explored DEM contact parameters of highly viscous soil particles by combining hysteretic spring and linear cohesion models, calibrated the coefficients of static friction and rolling friction, and verified accuracy of parameter calibration through field tests and simulation of ditching *(Aikins. et al., 2021)*. Xing et al. used the Hertz-Mindlin with JKR contact model in the simulation software extended discrete element model (EDEM) to calibrate key model parameters of lateritic soils in Hainan Province, China and obtained contact parameters between lateritic soil particles and between the soil and 28MnB5 plates. They also verified these parameters through tests of soil breakage resistance *(Xing et al., 2020)*. Taking soil around tubers during potato harvesting period as research objects, Li et al. calibrated the soil discrete element contact parameters through accumulation test and shear crushing test. The relative error between the simulation results and the actual measured values was 1.37% *(Li et al., 2022)*. Meanwhile, some scholars calibrated DEM parameters of specific soil according to research demands, including ploughed soil in a cotton field *(Song et al., 2021),* no-till soil in a winter wheat-corn rotation system *(Tian et al., 2021)*, grapevine anti-freezing soil *(Ma et al., 2020)*, covering soil on whole plastic film with mulching on double ridges *(Dai et al., 2019)*, and wet clayey paddy soil *(Ding et al., 2017)*. However, there is no research into the calibration of soil discrete element parameters in the planting area of rhizome medicinal materials in hilly region.

By combining simulation and physical tests, the discrete element parameters between soil and machine were calibrated. The angle of repose tests of soil could be conducted to calibrate contact parameters between soil particles and sliding tests of soil were conducted to calibrate contact parameters between soil and machinery. Furthermore, multivariate regression models of the contact parameters with the angles of repose and sliding were established, thus obtaining the optimal combination of contact parameters. Moreover, field tests and simulation were performed based on the self-developed rotary tillage and ridging machine to determine accurate and reliable DEM parameters of soil.

MATERIALS AND METHODS

Test materials

The test soil samples were collected from a planting area of *Fritillaria thunbergii* (Xinfeng Town, Dafeng District, Yancheng City, Jiangsu Province, China) (120°47′48″ N, 33°28′88″ E). The soil samples were collected in late May 2022, which was consistent with the harvesting period of *Fritillaria thunbergii*. Because *Fritillaria thunbergii* is a shallow-rooted crop, soils at the depth of 0~20 cm were taken as the research object. The field soil was sampled using the five-point sampling method, and test instruments were utilized to determine measure intrinsic parameters including the density, hardness, and moisture content. Afterwards, a cutting ring (100 cm^3) and an electronic balance (NS-3200A, measurement range of 0 to 3200 g, and precision of 0.001 g) were used to measure the soil density. A hardness meter of soil (TYD-2, measurement range of 100 kg, and precision of 0.5%) was employed to measure soil hardness in the plough layer. An electro-thermostatic blast oven (DHG-9076A, measurement range of 50 to 300 °C) was adopted to measure the average soil moisture content. The simulation parameters including shear modulus and Poisson's ratios of soil and steel components were derived from relevant literature (*Xing et al., 2020; Dai et al., 2019*). The specific parameters are listed in Table 1.

Table 1

Intrinsic physical parameters in DEM simulation of soil

Parameter	Value
Soil hardness [kPa]	1263.5
Soil moisture content	18.65%
Soil density [$kg \cdot m^{-3}$]	1250
Soil Poisson's ratio	0.4
Soil shear modulus [Pa]	1×10^6
Steel density [$kg \cdot m^{-3}$]	7.85×10^3
Steel Poisson's ratio	0.3
Steel shear modulus [Pa]	7×10^7

Physical tests of soil

The physical testing apparatus for the angle of repose of soil is shown in figure 1a. The apparatus consisted of a lifting test bench, a steel cylinder, and a steel plate. The steel cylinder had a height of 240 mm, a diameter of 80 mm, and a length-diameter ratio of 3:1, and its bottom was in contact with the steel plate (500 mm × 400 mm). The steel cylinder was filled with soil. Then, a KD-2768 hoisting machine was used to lift the cylinder at a constant rate of 0.02 m/s, which allowed soil particles to fall from the bottom of the cylinder and accumulate on the steel plate. After finishing each test, a digital display angle ruler (Kapro992, with a measurement range of 0° to ± 225°, and a precision of 0.05°) was used to measure the angle of repose θ from four directions (figure 1b) and the mean value in all four directions was taken as the value of the angle of repose of soil in the test. The test was repeated five times and the mean value was calculated. In this way, the angle of repose θ of soil was found to be 35.77°, with a standard deviation of 1.23° and a coefficient of variation (CV) of 3.44%.

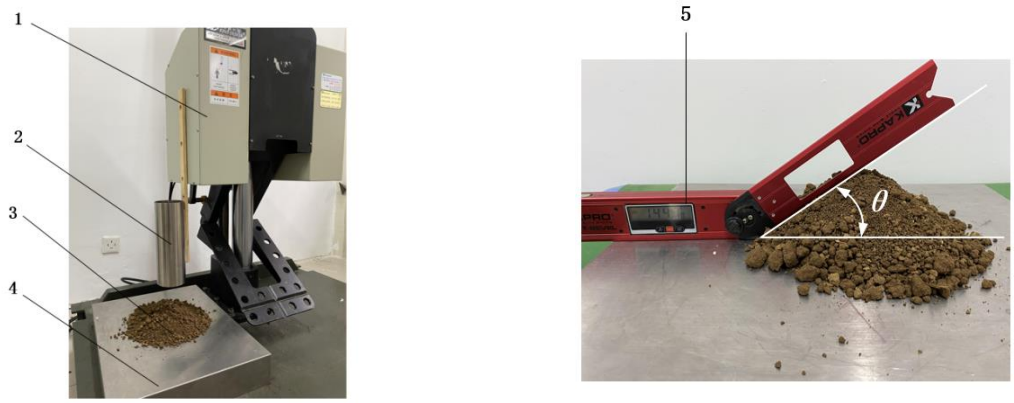

(a) Test bench for measuring the angle of repose of soil (b) Measurement of the angle of repose

Fig. 1 - Physical test of soil repose angle

1-Lifting test bench; 2 - Steel cylinder; 3 - Soil mound; 4 - Steel plate; 5 - Digital display angle ruler

The sliding tests of soil are shown in figure 2a. The test equipment comprised an inclined test bench, a steel box, a steel ring (Φ 154 mm × 30 mm), and a digital display angle ruler. The steel box was placed on the inclined test bench and leveled using the digital display angle ruler. The steel ring was put in the middle at the top of the steel box. Then, the electronic balance was used to weigh 100 g of soil, which were uniformly distributed around the steel ring. Afterwards, the steel ring was removed, and the inclined test bench was rotated around the y-axis at 2 °/s. The rotation was stopped when the soil began to slide. Under the condition, the digital display level ruler was used to measure the angle between the x-axis of the inclined test bench and the horizontal plane, that is, the sliding angle γ (Figure 2b). The test was repeated five times and the mean value was taken as the test result. In this way, the sliding angle γ of soil was found to be 22.4°, with a standard deviation of 0.41° and a CV of 1.35%.

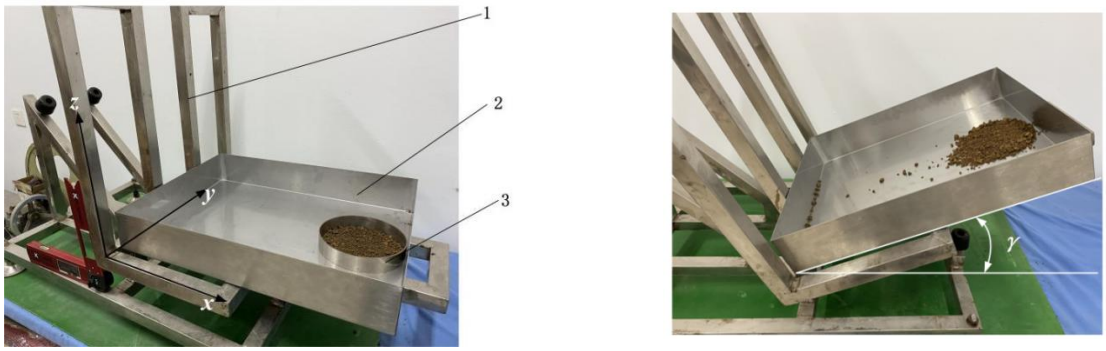

(a) Test bench for measuring the sliding angle of soil (b) Measurement of the sliding angle

Fig. 2 - Physical test of soil sliding angle

1- Inclined test bench; 2 - Steel box; 3 - Steel ring

DEM simulation of soil

(1) Determination of value ranges of parameters to be calibrated

The intrinsic parameters and simulation scale of soil and steel components were input to the EDEM software. Test factors and their value ranges in simulation were determined based on the GEMM (generic

EDEM material model) database and the literature (*Aikins. et al., 2021; Tian et al., 2021; Song et al., 2021*). The value ranges of factors A (the coefficient of restitution of soil particles), B (coefficient of static friction of soil particles), C (the coefficient of rolling friction of soil particles), D (JKR surface energy), E (coefficient of restitution between soil and steel), F (the coefficient of static friction between soil and steel), and G (the coefficient of rolling friction between soil and steel) are 0.15 to 0.75, 0.2 to 1.16, 0.05 to 0.25, 0.01 to 2.8 J/m^2, 0.05 to 0.65, 0.3 to 0.9, and 0.05 to 0.25, respectively.

(2) Establishment of the simulation model

According to the simulation scale, the built-in spherical particle elements of EDEM were used to establish the soil model and set the radius of soil particles and the magnifying power of spherical diameter as 5 mm and 0.95 to 1.05, respectively *(Shi et al., 2017)*. The three-dimensional (3-d) models of the test benches for the angle of repose tests and sliding tests of soil were built using SolidWorks, saved as .x_t format, and imported in EDEM. As shown in Figure 3 and Figure 4, the simulation models were simplified: only the cylinder and steel plate were reserved in the angle of repose tests of soil and only the steel box was reserved in the sliding tests, whose sizes were same as those of the cylinder, steel plate, and steel box in the physical tests of soil. The cylinder in the angle of repose tests was lifted at 0.02 m/s and the steel box in the sliding tests was rotated at 2 °/s, all consistent with those in the physical tests of soil. The intrinsic parameters of soil and steel components were set as Table 1. The Hertz-Mindlin with JKR contact model was selected for soil particles, and the Hertz-Mindlin non-sliding contact model was selected for soil particles and steel components. The time step in Rayleigh analysis was set to 20%. In addition, the interval for data storage, gravitational acceleration, and grid cell size were 0.01 s, 9.81 m/s^2, and 2.5 times the average radius of particles, respectively.

After completing the simulation, the model was adjusted to the front view and images were captured. In order to avoid the result error caused by human measurement, the repose angle measurement adopts the method of image processing (Figure 4). The image was captured as 804×804 pixels and imported into MATLAB. Firstly, the RGB original image was converted into a binary image, and the left half of the binary image was obtained by image segmentation. Then the boundary curve was extracted by edge detection, and the fitting line was further obtained. The angle between the fitting line and the horizontal plane is the repose angle. The slip angle was obtained by measuring the angle between the flat plate and the horizontal plane by CAD software.

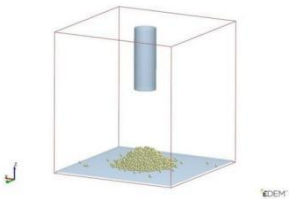

(a) Simulation model of the angle of repose test of soil

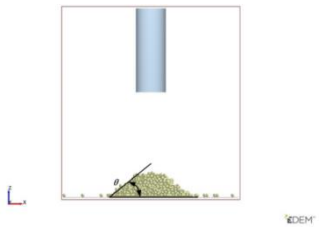

(b) Simulation results of the angle of repose

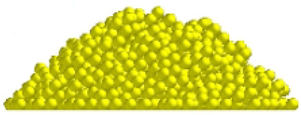

(c) RGB original image

(d) binary image

(e) half of the binary image

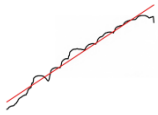

(f) boundary curve and fitting line

Fig. 3 - Simulation of the angle of repose of soil

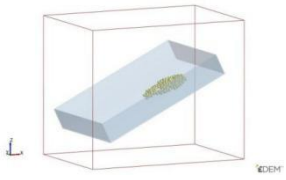

(a) Simulation model of the sliding angle test of soil

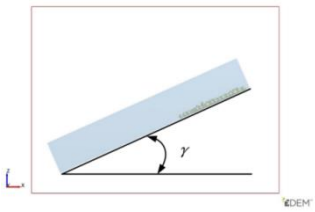

(b) Simulation results of the sliding angle

Fig. 4 - Simulation of the sliding angle of soil

(3) Arrangement of simulation

The contact parameters (A, B, C, and D) of soil particles were calibrated by conducting simulation on the angle of repose of soil, and those between soil and steel (E, F, and G) were calibrated through simulation

of the sliding angle. At first, the steepest ascent experiments were designed to shrink the ranges of values of parameters, to approach the optimal values with greatest accuracy. In the simulation, the parameter values were increased at the designed steps and the corresponding angles of repose and sliding of soil in the simulation were recorded and analyzed.

Parameters were set to three levels (high, intermediate, and low which were separately expressed as +1, 0, and −1) according to results of the steepest ascent experiments and the Box-Behnken test design. The error was estimated using five central points in the tests, in which 29 and 17 groups of simulation were separately conducted on the angles of repose and sliding of soil, during which these were measured for specimens in each group and were recorded. Then, analysis of variance (ANOVA) was applied to the simulation results and the multivariate regression analysis was used to obtain regression models. By using the parameter optimization module in Design-Expert, the established models were optimized taking the repose and sliding angles of soil as the objectives, so as to determine the optimal solutions. Thereafter, the simulation results were verified.

Test verification of rotary tillage and ridging work

(1) Field tests of rotary tillage and ridging work

The rotary tillage and ridging machine mainly consisted of a caterpillar chassis, a suspension system, a gear reducer, a chain driving system, a rotary tillage and ditching device, a ditch-cleaning shovel, a ridge roller, and a rack. The whole machine is shown in Figure 5a and the main technical parameters are listed in Table 2. The tests were conducted in the planting area of *Fritillaria thunbergii* (Xinfeng Town, Dafeng District, Yancheng City, Jiangsu Province) after harvest.

Main technical parameters of the whole machine **Table 2**

Parameter	Value
Overall machine size [mm × mm × mm]	4950 × 2030 × 2020
Total mass [kg]	2618
Matched power [kW]	36.8
Knife-cylinder speed [rpm]	230
Rotational speed of ridge roller [rpm]	85

According to the test method stipulated in the Rototill combine equipment Part 2: Rototill scarifying-paring-ridging machine (JB/T8401.2-2017), the machine was driven in a field. This formed three complete ridges and two half ridges. The forward speed, rotational speed of rotary blades, tillage depth of the machine, and rotational speed of the ridge roller were 0.5 m/s, 230 rpm, 220 mm, and 85 rpm, respectively. Field tests are shown in Figure 5b. The measurement devices included a leather measuring tape, a steel measuring tape, and a digital display level ruler (KAPRO-985D with a measurement range of 0 to 180°, and a precision of 0.1°). The sections with the length of 20 m in the middle of the three complete ridges were taken as the data measurement ranges. The ridge height, top width of ridges, and bottom width of ditches were measured by using the five-point sampling method and then they were recorded.

(a) Test prototype

(b) Operation effect

(c) Measurement of ridge height

(d) Measurement of top width of ridges and bottom width of ditches

Fig. 5 - Field tests of rotary tillage and ridging work

(2) Simulation of rotary tillage and ridging work

The geometries module in EDEM was used to establish the soil-bin model measuring 2100 mm × 2100 mm × 400 mm, and SolidWorks was adopted to build the 3D model of the rotary tillage and ridging machine. The models were simplified and then imported in EDEM (figure 6). Soil particles were set using the calibrated and optimized parameters, and the Hertz-Mindlin non-sliding contact model was applied between the soil and rotary tillage ridging parts. Based on relevant research results and combining with the simulation scale, the radius of soil particles was magnified to 10 mm, which can effectively save simulation resources and improve the simulation efficiency (*Dai et al., 2019*).

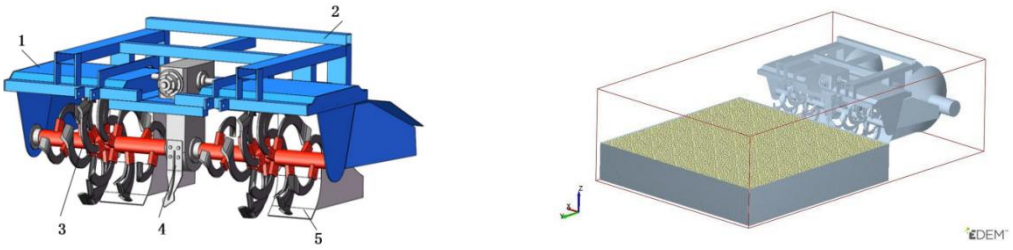

(a)3-d model of the rotary tillage and ridging machine (b)DEM model of rotary tillage and ridging work

Fig. 6 - Simulation models of rotary tillage and ridging machine and work
1- Cover plate; 2 - Rack; 3 - Rotary blade; 3 - Small front plough; 3 - Trenching shovel

The rotational speed of rotary blades, forward speed of the machine, tillage depth, and rotational speed of the ridge roller were the same as those in the field tests. After simulation, the ridge height (h), top width of ridges (l_1), bottom width of ditches (l_2) was measured at five points in the stable working stage and their averages were calculated, as shown in figure 7. The deviations were calculated using equation 1.

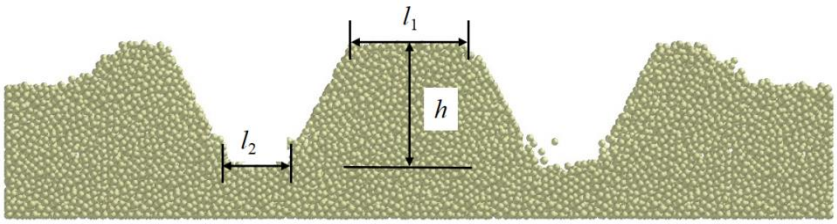

Fig. 7 - Measurement in the simulation of rotary tillage and ridging work

$$\delta = \frac{|\eta' - \eta|}{\eta} \times 100\% \quad (1)$$

where η' and η represent the simulation and field test results of the ridge height, top width of ridges, and bottom width of ditches, respectively.

RESULTS

Results of the steepest ascent experiments

The steepest ascent experiments were conducted taking the JKR surface energy, contact parameters of soil particles, and contact parameters between soil and steel as test factors. The relative errors of the actual repose and sliding angles with the simulation results were calculated. Simulation results of the angle of repose are listed in Table 3.

Table 3

Results of steepest ascent experiments of the angle of repose

Serial Number	Parameter A	Parameter B	Parameter C	Parameter D [J·m^{-2}]	Angle of repose θ [°]	Relative error
1	0.15	0.2	0.05	0.01	9.83	-72.52%
2	0.3	0.44	0.1	0.7	33.93	-5.14%
3	0.45	0.68	0.15	1.4	37.52	4.89%
4	0.6	0.92	0.2	2.1	40.05	11.97%
5	0.75	1.16	0.25	2.8	90	151.61%

In the third group of tests, the relative error of the angle of repose is the minimum of 4.89%, so it is determined that the optimal interval is approximated to the third group of parameters.

Therefore, the subsequent Box-Behnken tests were conducted by taking the parameter values in the third group as the intermediate level, and those in the second and fourth groups as the low and high levels. Simulation results of the sliding angle are listed in Table 4. In the second group of tests, the relative error of the sliding angle is minimized, so the optimal interval is found to be approximated to the second group of parameters. Hence, the subsequent Box-Behnken tests were conducted by taking the parameter values in the second group as the intermediate level, and those in the first and third groups as the low and high levels.

Table 4

Results of steepest ascent experiments of the sliding angle

Serial Number	Parameter E	Parameter F	Parameter G	Sliding angle γ [°]	Relative error
1	0.05	0.3	0.05	16.88	-24.64%
2	0.2	0.45	0.1	23.77	6.12%
3	0.35	0.6	0.15	27.15	21.21%
4	0.5	0.75	0.2	32.12	43.39%
5	0.65	0.9	0.25	37.35	66.74%

Box-Behnken test results of the angle of repose

Table 5 lists the Box-Behnken test results of the angle of repose. The multivariate regression model between the angle of repose θ of soil particles and various contact parameters was constructed using Design-Expert based on the test results and the polynomial equation is shown as equation 2.

Table 5

Box-Behnken test results of the angle of repose

Serial Number	Parameter A	Parameter B	Parameter C	Parameter D [J·m^{-2}]	Angle of repose θ [°]
1	-1 (0.3)	-1 (0.44)	0 (0.15)	0 (1.4)	32.15
2	1 (0.6)	-1	0	0	36.1
3	-1	1 (0.92)	0	0	36.85
4	1	1	0	0	36.99
5	0 (0.45)	0 (0.68)	-1 (0.1)	-1 (0.7)	32.16
6	0	0	1 (0.2)	-1	39.65
7	0	0	-1	1 (2.1)	41.27
8	0	0	1	1	37.6
9	-1	0	0	-1	34.73
10	1	0	0	-1	35.7
11	-1	0	0	1	37.45
12	1	0	0	1	39.78
13	0	-1	-1	0	37.12
14	0	1	-1	0	38.56
15	0	-1	1	0	37.83
16	0	1	1	0	39.65
17	-1	0	-1	0	35.08
18	1	0	-1	0	38.97
19	-1	0	1	0	37.98
20	1	0	1	0	38.82
21	0	-1	0	-1	32.92
22	0	1	0	-1	35.8
23	0	-1	0	1	37.81
24	0	1	0	1	39.2
25	0	0	0	0	36.16
26	0	0	0	0	36.86
27	0	0	0	0	36.24
28	0	0	0	0	36.43
29	0	0	0	0	36.01

$$\theta = 36.34 + 1.01A + 1.09B + 0.7C + 1.85D - 0.95AB + -0.76AC + 0.34AD + 0.095BC - 0.37BD - 2.79CD - 0.19A^2 - 0.14B^2 + 1.58C^2 + 0.25D^2 \quad (2)$$

The coefficient of determination R^2, corrected determination coefficient A_{dj} R^2, and CV of the regression equation are 0.9541, 0.9083, and 1.81%, respectively. The result implies that the regression model has a high degree of fitting and favorable correlations, so it can be used for further analysis. By ANOVA in regression of test results (Table 6), the regression model is found to have $P < 0.0001$, which indicates that the model is very significant and can be used to estimate the angle of repose of soil.

Among these four test factors, A, B, C, and D all have significant influences on the angle of repose of soil, and they are listed (in ascending order) as B, D, A and C according to their significance. AB and AC have a significant effect on the angle of repose, CD has an extremely significant effect on the angle of repose, and the interaction of other factors is not significant. Except for C^2 that has extremely significant influences of the angle of repose, quadratic items of other factors have insignificant influences.

Table 6

ANOVA of the regression equation of the angle of repose of soil

Sources of variation	Sum of squares	Degree of freedom	Mean square	F	P
Model	130.07	14	9.29	20.81	< 0.0001
A	12.24	1	12.24	27.42	0.0001
B	14.34	1	14.34	32.13	< 0.0001
C	5.84	1	5.84	13.08	0.0028
D	40.89	1	40.89	91.58	< 0.0001
AB	3.63	1	3.63	8.13	0.0128
AC	2.33	1	2.33	5.21	0.0386
AD	0.46	1	0.46	1.04	0.3261
BC	0.036	1	0.036	0.081	0.7803
BD	0.56	1	0.56	1.24	0.2836
CD	31.14	1	31.14	69.74	< 0.0001
A2	0.22	1	0.22	0.5	0.4913
B2	0.12	1	0.12	0.28	0.6073
C2	16.11	1	16.11	36.08	< 0.0001
D2	0.4	1	0.4	0.9	0.3599
Residual	6.25	14	0.45		
Lack of Fit	5.82	10	0.58	5.42	0.0589
Pure Error	0.43	4	0.11		
Cor Total	136.32	28			

The regression model of the angle of repose was optimized using the parameter optimization module in Design-Expert and taking the angle of repose of 35.77° as the objective. The resulting sets of solutions were used to simulate and verify the angle of repose. By doing so, a set of optimal solutions enabling a shape similar to that in physical tests was obtained, including A (coefficient of restitution of soil particles) of 0.57, B (coefficient of static friction of soil particles) of 0.85, C (the coefficient of rolling friction of soil particles) of 0.15, and D (JKR surface energy) of 1.05 J/m^2.

Box-Behnken test results of the sliding angle

Table 7 lists the Box-Behnken test results of the sliding angle. According to the test results, Design-Expert was used to establish the multivariate regression model of the sliding angle γ with various contact parameters of soil particles and the polynomial equation is expressed as equation 3.

Table 7

Box-Behnken test results of the sliding angle

Serial Number	Parameter E	Parameter F	Parameter G	Sliding angle γ [°]
1	-1 (0.05)	-1 (0.3)	0 (0.1)	18.66
2	1 (0.35)	-1	0	18.56
3	-1	1 (0.6)	0	23.16
4	1	1	0	23.13
5	-1	0 (0.45)	-1 (0.05)	14.95
6	1	0	-1	14.23
7	-1	0	1 (0.15)	23.62
8	1	0	1	23.89
9	0 (0.2)	-1	-1	10.15
10	0	1	-1	18.11
11	0	-1	1	24.37
12	0	1	1	23.89
13	0	0	0	22.04
14	0	0	0	21.7
15	0	0	0	21.63
16	0	0	0	22.06
17	0	0	0	22.29

$$\gamma = 21.94 - 0.072E + 2.07F + 4.79G + 0.017EF + 0.25EG - 2.11FG - 0.51E^2 - 0.55F^2 - 2.26G^2 \quad (3)$$

The coefficient of determination R^2, corrected determination coefficient A_{dj} R^2, and CV of the regression equation are 0.9963, 0.9915, and 1.83%, respectively, indicative of a high goodness of fit and close correlations in the regression model, so it can be used in subsequent analysis. Through ANOVA in regression of test results (Table 8), the regression model is found to have P < 0.0001, which indicates that the model is very significant and can be used to estimate the sliding angle of soil. Among the above three test factors, F and G have extremely significant influences while E exerts no significant influences on the sliding angle of soil; FG has extremely significant influences on the sliding angle, while the interaction of other factors exerts insignificant influences. E^2 and F^2 have significant influences while G^2 has extremely significant influences on the sliding angle of soil.

Table 8

ANOVA of the regression equation of the sliding angle of soil on steel components

Sources of variation	Sum of squares	Degree of freedom	Mean square	F	P
Model	261.29	9	29.03	207.81	< 0.0001
E	0.042	1	0.042	0.3	0.6003
F	34.24	1	34.24	245.07	< 0.0001
G	183.65	1	183.65	1314.53	< 0.0001
EF	0.00123	1	0.00123	0.00877	0.928
EG	0.25	1	0.25	1.75	0.227
FG	17.81	1	17.81	127.47	< 0.0001
E2	1.1	1	1.1	7.9	0.0261
F2	1.29	1	1.29	9.27	0.0187
G2	21.5	1	21.5	153.87	< 0.0001
Residual	0.98	7	0.14		
Lack of Fit	0.68	3	0.23	3.01	0.1577
Pure Error	0.3	4	0.075		
Cor Total	262.26	16			

By using the parameter optimization module in Design-Expert, the regression model of the sliding angle was optimized taking the sliding angle of 22.4° as the objective. The resulting sets of solutions were used to simulate and verify the sliding angle. In this way, a set of optimal solutions enabling a shape similar to that in physical tests could be obtained, including E (coefficient of restitution between soil and steel) of 0.09, F (coefficient of static friction between soil and steel) of 0.5, and G (coefficient of rolling friction between soil and steel) of 0.09.

Test verification results of the repose and sliding angles

To verify the accuracy of the contact model of soil and the calibration results of contact parameters, DEM simulation was carried out on the repose and sliding angles and the test results are shown in Figure 8 and Figure 10. Each test was repeated for five times.

The angle of repose of soil was 37.18° and the sliding angle of soil on the steel was 23.22°. Compared with the physical tests, the errors were separately 3.94% and 3.66%, indicating the accuracy and reliability of the calibrated parameters.

(a) Physical test of the angle of repose of soil (b) Simulation of the angle of repose of soil

Fig. 8 - Comparison of physical tests and simulation of the angle of repose of soil

(a) Initial sliding state (b) Complete sliding state

Fig. 9 - Physical tests of the sliding angle of soil. (a) Initial sliding state; (b) Complete sliding state

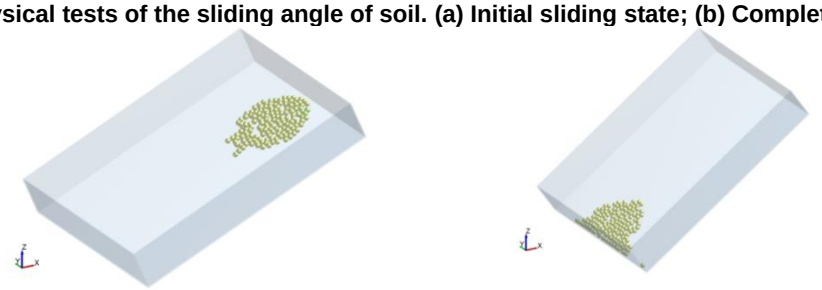

(a)Initial sliding state; (b)Complete sliding state

Fig. 10 - Simulation of the sliding angle of soil. (a) Initial sliding state; (b) Complete sliding state

Simulation of rotary tillage and ridging work

Figure 11 shows the rotary tillage and ridging process of the rotary tillage and ridging machine under the optimal combination of calibrated contact parameters between soil particles and geometries. The 0.4 s before simulation covered the contact process between rotary tillage and ridging components and soil, and soil particles migrated under action of rotary blades at 0.4 s; from 0.4 to 1.6 s, soil particles were cut and smashed under the action of rotary blades and thrown to the bonnets and soil-retaining boards in both sides with the high-speed rotation of the shaft of rotary blades; at 2.8 s, the rotary tillage and ridging machine was in complete contact with the soil particles, and the soil particles below the soil-retaining boards were extruded to ridges under the action of the ridge roller; from 2.8 to 4.0 s, the rotary tillage and ridging machine tended to work steadily and obvious ridges were formed on the soil surface.

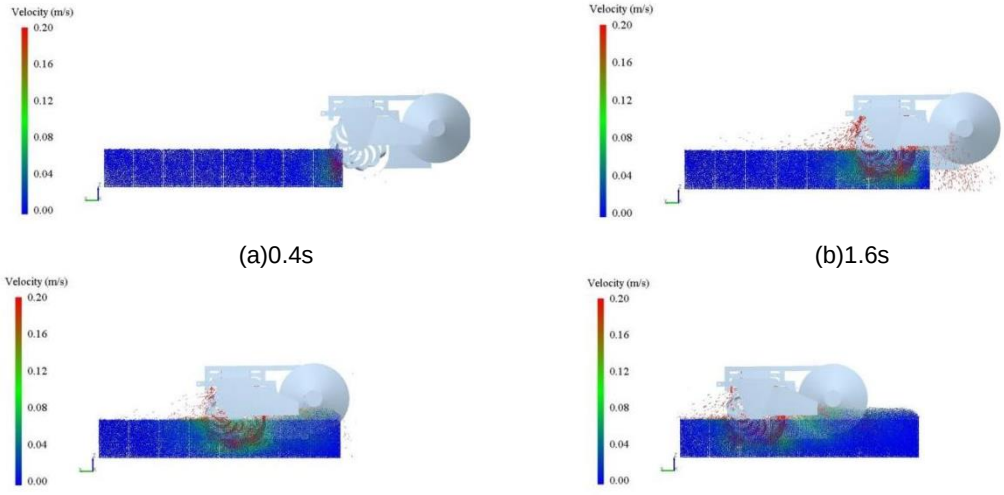

(a)0.4s (b)1.6s

(c)2.8s (d)4.0s

Fig. 11 - Simulation of rotary tillage and ridging work

Field test and simulation results of rotary tillage and ridging work are displayed in Table 9. The ridge height, top width of ridges, and bottom width of ditches in the field tests are 334.6, 326.3, and 158.8 mm, respectively; while those in simulation are 319.7, 303.6, and 145.2 mm. The two have relative errors of 4.45%, 6.96%, and 8.56% (all less than 10%), indicative of the accuracy of the simulation. The test results show that after calibrating and optimizing DEM model parameters using the multivariate regression model based on the JKR contact model and combining with value ranges of physical parameters recommended by the GEMM database of EDEM, rotary tillage ridging parts move in a same way in the simulated soil model as that in the field tests. The result indicates that the calibration and optimization of relevant contact parameters are reliable and effective.

Table 9

Comparison of simulation and field test results of rotary tillage and ridging work

Parameter	Field test result	Simulation result	Relative error
Ridge height [mm]	334.6	319.7	4.45%
Top width of ridges [mm]	326.3	303.6	6.96%
Bottom width of ditches [mm]	158.8	145.2	8.56%

CONCLUSIONS

The soil in the planting area of *Fritillaria thunbergii* was taken as the research object. The Hertz-Mindlin with JKR model was selected as the contact model to calibrate contact parameters between soil particles and between soil and steel through the combination of physical tests and simulation. The optimal combination of parameters was determined, which was verified by comparing field tests and simulation of rotary tillage and ridging work. The main conclusions obtained are as follows:

The multivariate regression model of the angle of repose was established using the Box-Behnken optimization method taking the coefficient of restitution of soil particles, the coefficient of static friction and the coefficient of rolling friction, and JKR surface energy of soil particles as test factors and the simulated angle of repose as the evaluation index of tests. Through optimization, the coefficients of restitution of soil particles, static friction and rolling friction, and JKR surface energy of soil particles were 0.57, 0.85, 0.15, and 1.05 J/m^2, respectively. Under the optimal solution, the simulated angle of repose is 37.18°, which has a relative error of 3.94% with the physical tests.

Soil sliding tests were conducted to calibrate and optimize the coefficients of restitution, static friction and rolling friction between soil and steel. Taking the sliding angle of soil as the evaluation index of tests, the multivariate regression model of the sliding angle was established using the Box-Behnken optimization method. Through optimization, the coefficients of restitution, static friction and rolling friction between soil and steel were obtained as 0.09, 0.5, and 0.09, respectively. The simulation result of the static sliding friction angle in the optimal solution is 23.22°, which has a relative error of 3.66% with the physical tests.

To verify the accuracy of the calibrated and optimized DEM model parameters, field tests and simulation of rotary tillage and ridging work were conducted and compared. The simulation can characterize soil migration in the rotary tillage and ridging process. The measurement results of the ridge height, top width of ridges, and bottom width of ditches in the simulation show errors of 4.45%, 6.96%, and 8.56% compared to those in field tests, that is, all relative errors are below 10%, within an acceptable range. The result indicates that simulation model of soil shares consistent physico-mechanical properties with the actual soil, verifying the accuracy and reliability of calibration results of DEM simulation parameters and the research method on planting area soil of rhizome medicinal materials. The research explored the method for systematic calibration and optimization of physical parameters of soil in DEM simulation and established the accurate DEM simulation model for planting area soil of rhizome medicinal materials in hilly region. It can provide theoretical basis and technical support for soil - machine interaction research and machine design.

ACKNOWLEDGEMENT

This research was funded by Institute-level basic scientific research business expenses project of the Chinese Academy of Agricultural Sciences (S202101-03, S202218, S202219). We greatly appreciate the careful and precise reviews by the anonymous reviewers and editors.

REFERENCES

[1] Aikins, K. A., Ucgul, M., Barr, J. B., Jensen, T. A., Antille, D. L., Desbiolles, J. M. (2021). Determination of discrete element model parameters for a cohesive soil and validation through narrow point opener performance analysis. *Soil and Tillage Research*, Elsevier/Amsterdam, Vol.213, ISSN 0167-1987, 105123.

[2] Chen, Y., Munkholm, L. J., Nyord, T. (2013). A discrete element model for soil–sweep interaction in three different soils. Soil Tillage Res, 2013, 126, 34-41. *Soil and Tillage Research*, Elsevier/Amsterdam, Vol.126, pp.34-41.

[3] Chen, Y.; Zou, J.; Sun, H.; Qin, J.; Yang, J. (2021). Metals in traditional Chinese medicinal materials (TCMM): A systematic review. *Ecotoxicology and Environmental Safety*, Elsevier/Amsterdam, Vol.207.

[4] Dai, F.; Song, X.; Zhao, W.; Zhang, F.; Ma, H.; Ma, M. (2019). Simulative Calibration on Contact Parameters of Discrete Elements for Covering Soil on Whole Plastic Film Mulching on Double Ridges (全膜双垄沟覆膜土壤离散元接触参数仿真标定). *Transactions of the Chinese Society of Agricultural Engineering*, Chaoyang / Beijing, vol. 50 No. 2, ISSN 1002-6819, pp. 49-56+77.

[5] Ding, Q.; Ren, J.; Belal, E.; Zhao, J.; Ge, S.; Li, Y. (2017) DEM Analysis of Subsoiling Process in Wet Clayey Paddy Soil (湿粘水稻土深松过程离散元分析). *Transactions of the Chinese Society of Agricultural Engineering*, Chaoyang / Beijing, vol. 48 No. 3, ISSN 1002-6819, pp. 38-48.

[6] Huang, L. (2021). National Chinese Medicinal Materials Production Statistics Report (2020). Shanghai Science and Technology Press: Shanghai, China.

[7] Li, Y.; Fan, J.; Hu, Z.; Luo, W.; Yang, H.; Shi, L.; Wu, F. (2022) Calibration of Discrete Element Model Parameters of Soil around Tubers during Potato Harvesting Period. *Agriculture*, MDPI/Basel, Vol.12.

[8] Ma, S.; Xu, L.; Yuan, Q.; Niu, C.; Zeng, J.; Chen, C.; Wang, S.; Yuan, X. (2020) Calibration of discrete element simulation parameters of grapevine anti-freezing soil and its interaction with soil-cleaning components (葡萄藤防寒土与清土部件相互作用的离散元仿真参数标定). *Transactions of the Chinese Society of Agricultural Engineerin*g, Chaoyang / Beijing, vol.36, No.1, ISSN 1002-6819, pp. 40-49.

[9] Shi, L.; Zhao, W.; Sun, W. (2017). Parameter calibration of soil particles contact model of farmland soil in northwest arid region based on discrete element method (基于离散元的西北旱区农田土壤颗粒接触模型和参数标定). *Transactions of the Chinese Society of Agricultural Engineering*, Chaoyang / Beijing, vol.33, No.21, pp. 181-187.

[10] Song, S.; Tang, Z.; Zheng, X.; Liu, J.; Meng, X.; Liang, Y. (2021). Calibration of the discrete element parameters for the soil model of cotton field after plowing in Xinjiang of China (新疆棉田耕后土壤模型离散元参数标定). *Transactions of the Chinese Society of Agricultural Engineering*, Chaoyang / Beijing, vol.37, No.20, pp. 63-70.

[11] ***The Ministry of Industry and Information Technology of the People's Republic of China. *Rototill combine equipment Part 2: Rototill scarifying-paring-ridging machine: JB/T 8401.2-2017*; Machinery Industry Press: Beijing,

[12] Tian, X.; Cong, X.; Qi, J.; Guo, H.; Li, M.; Fan, X. (2021). Parameter Calibration of Discrete Element Model for Corn Straw-Soil Mixture in Black Soil Areas (黑土区玉米秸秆-土壤混料离散元模型参数标定). *Transactions of the Chinese Society of Agricultural Engineering*, Chaoyang/Beijing, vol. 52 No.10, pp.100-108+242.

[13] Ucgul, M.; Saunders, C. (2020). Simulation of tillage forces and furrow profile during soil-mouldboard plough interaction using discrete element modelling. *Biosystems Engineering*, Elsevier/Amsterdam, Vol.190, pp.58-70.

[14] Xing, J.; Zhang, R.; Wu, P.; Zhang, X.; Dong, X.; Chen, Y.; Ru, S. (2020). Parameter calibration of discrete element simulation model for latosol particles in hot areas of Hainan Province (海南热区砖红壤颗粒离散元仿真模型参数标定). *Transactions of the Chinese Society of Agricultural Engineering*, Chaoyang / Beijing, vol.36, No.5, pp. 158-166.

[15] Zhao, Z.; Guo, P.; Brand, E. (2012). The formation of daodi medicinal materials. *Journal of Ethnopharmacology*, Elsevier/Amsterdam, Vol.140, pp.476-481.